Accumulated photon echo in ruby and alexandrite

M. H. F. Overwijk, P. J. Rump, J. I. Dijkhuis, and H. W. de Wijn
Faculty of Physics and Astronomy, and Debye Research Institute, University of Utrecht, P.O. Box 80000, 3508 TA Utrecht, The Netherlands
(Received 23 October 1990; revised manuscript received 5 April 1991)

The technique of picosecond accumulated photon echo is applied to 700-at. ppm ruby and 2000-at. ppm alexandrite. The decay of the photon-echo intensity versus the probe-pulse delay displays a beat. A detailed analysis on the basis of Bloch equations shows that the beat frequency is associated with the zero-field splitting of the $^4A_2$ ground state, and that its phase and amplitude are determined by the amount of population communication within this state. Precise values for the spontaneous decay time of $2\overline{A}(^2E)$ and the $^4A_2$ zero-field splitting are derived.

I. INTRODUCTION

The technique of accumulated photon echo[1] has proved to be a powerful tool to measure phase relaxation with minimal disturbance of the system under study. The basic idea is that the effects of successive pairs of weak pump and probe pulses are integrated over times as long as the radiative lifetime. In this paper, we apply the technique of picosecond accumulated photon echo on the $^4A_2$-$\overline{E}(^2E)$ and $^4A_2$-$2\overline{A}(^2E)$ transitions of Cr^{3+} in 700-at. ppm ruby and 2000-at. ppm alexandrite at 1.5 K. In doing so, we demonstrate that accumulated photon echo can also serve to determine small level splittings with high accuracy. In the present case, this feature is used to measure the $^4A_2$ ground-state splitting of Cr^{3+}. The splitting is reflected in an oscillatory dependence of the echo intensity on the delay between the pump and the probe pulses. As is shown in a detailed analysis in terms of Bloch equations for an appropriate three-level system in interaction with the laser field, the beat in the echo can be ascribed to interference between the microscopic polarizations associated with the two transitions from the split ground level to the upper level. The beat also allows us to establish a lower limit for the rate of population communication within the ground state.

II. EXPERIMENTAL DETAILS

In the technique of accumulated photon echo,[1] a train of optical pulse pairs is applied to an ensemble of two-level systems ("dipoles"), and the effect of the successive pulse pairs is stored in a spectral, and for that matter spatial, grating. The first, or pump, pulse of each pair excites all dipoles to some extent, but the resultant macroscopic polarization rapidly decays as a result of dephasing caused by the inhomogeneity in the resonance frequencies. The microscopic polarization, however, only decays on the much longer time scale of the homogeneous dephasing time. After a variable delay, the microscopic polarization is probed by a second, or probe, pulse. Depending on the current phase, i.e., the frequency, of the particular dipole, the probe pulse either increases or decreases the amount of excitation. Accumulation of the effects produced by a single pulse pair over times as long as the radiative lifetime then results in a population grating extending over the width of the inhomogeneously broadened absorption line. The grating is read out by the next pulse pair. The next pump pulse induces constructive interference between the radiating dipoles in such a way that, in contrast to regular two-pulse photon echo, the macroscopic polarization reappears at the time of the next probe pulse. The accumulation and further constructive interference associated with the geometry lead to considerable enhancement of the signal intensity.

The experimental setup includes a dye laser operating with pyridine-1 dye, pumped by a mode-locked Ar-ion laser. It produces Fourier-limited 10-ps pulses at a wavelength around 690 nm, as appropriate for excitation of Cr^{3+} in sapphire (ruby, 693 nm) and chrysoberyl (alexandrite, 679 nm) at 1.5 K. The repetition rate of the pulses is 82 MHz, and the average output power typically 20 mW, which is intense enough to excite both transitions departing from the ground state. The beam is split into two beams of equal intensity, which are subsequently directed towards the sample in the cryostat at a mutual angle of approximately 3° of arc. The beams are focused on the same spot in the sample, one of the beams being delayed by up to 3 ns with an optical delay line. The polarization was chosen at such an angle with the c axis that maximum echo intensity of the $^4A_2$-$2\overline{A}(^2E)$ transition was obtained. This angle is determined by the transition probabilities[2] on the one hand and ground-state depletion by the optical pumping cycle on the other. After passing through the sample, the probe pulse inclusive of the echo signal is spatially selected by the use of a pin hole, and detected with a photodiode.

To enhance the signal-to-noise ratio, we employed a double-modulation technique, in which the pump and probe beams are modulated electro-optically, the pump beam at a frequency of 10 MHz, and the probe beam at a frequency which is slow with respect to the radiative decay of the upper level. The rf voltage from the photo-

diode is amplified with a narrow-band amplifier tuned to 10 MHz. The signal, still containing both modulation frequencies, is subsequently phase-sensitively demodulated with respect to the 10-MHz reference oscillator, and then demodulated with respect to the audio frequency. The resulting signal is fed to an analog-to-digital converter for further processing.

III. EFFECTS OF GROUND-STATE SPLITTING

A. Three-level scheme

To investigate the effects on the photon echo of a ground state which is split into two well-separated components, we consider a three-level system with the two lowest-lying levels close together [Fig. 1(a)]. In the case of ruby, these two levels are to be identified with the $M_S = \pm\frac{3}{2}$ and $\pm\frac{1}{2}$ Kramers doublets of $^4A_2$, and the top level with $\overline{E}(^2E)$. With suitable modifications allowing for the removal of active centers from the top level in between pulse pairs,[1] however, the results equally apply to $2\overline{A}(^2E)$.

A single near-resonant optical field excites both ground-state components to the upper level [Fig. 1(a)], but the two transitions have different detunings from resonance,

$$\Delta_1 = (E_c - E_a)/\hbar - \omega_L \ , \qquad \Delta_2 = (E_c - E_b)/\hbar - \omega_L \ , \tag{1}$$

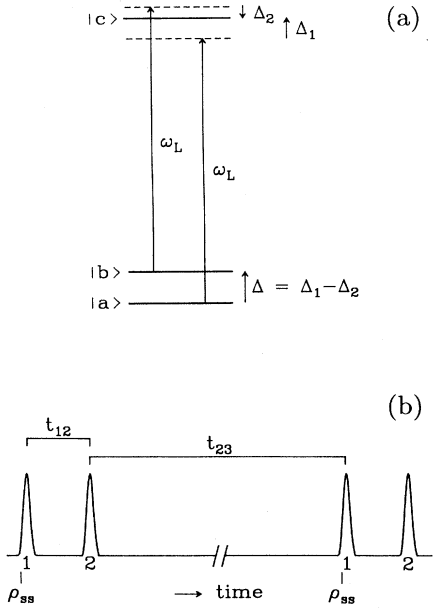

FIG. 1. (a) The three-level scheme accounting for the beat in the echo intensity due to a split ground state. Indicated are the optical driving field at angular frequency ω_L, and the detunings from resonance Δ_1 and Δ_2. (b) The pulse sequence in an accumulated-photon-echo experiment.

where E_a, E_b, and E_c are the energies of the levels, and ω_L is the angular frequency of the optical field. The total detuning $\Delta_1 - \Delta_2$, of course, equals the ground-state splitting Δ, which is assumed not to vary from site to site. This assumption is justified by the small width of the electron spin resonance transition within $^4A_2$, and the negligible decay of the accumulated photon echo on the $^4A_2$-$\overline{E}(^2E)$ transition (cf. the upper frames of Figs. 6 and 7 below).

The total Hamiltonian of the three-level system is given by $H_0 + H_I + H_R$, where H_0 is the Hamiltonian of the noninteracting system, H_I describes the interaction with the laser field, and H_R accounts for the relaxation.[3] The Hamiltonian H_I can be written

$$H_I = -\boldsymbol{\mu} \cdot \mathbf{E}_0(t) \cos(\omega_L t - \mathbf{k} \cdot \mathbf{r} + \phi) \ , \tag{2}$$

in which $\mathbf{E}_0(t)$, $\mathbf{k}$, and ϕ are the amplitude, wave vector, and phase of the laser field, respectively. The electric dipole moment $\boldsymbol{\mu}$ is assumed to be the same for the two optical transitions. This is a reasonable assumption for the given light polarization (Sec. II); no direct laser-field-induced matrix elements connect the two components of the ground state. To describe the density matrix ρ specifying the three-level system $|a\rangle$, $|b\rangle$, $|c\rangle$ as it develops when subjected to the part $H_0 + H_I$, we rely on the Liouville variant of the Schrödinger equation, $i\hbar\dot{\rho} = [H, \rho]$. The effects of H_R are subsequently introduced in the customary heuristic way by adding appropriate single-exponential decay terms to the equations of motion of the various elements of ρ.

It is useful to go over to a reference frame rotating with the frequency of the exciting field by the use of

$$\tilde{\rho}_{ac} = \rho_{ac} e^{-i\omega_L t}, \quad \tilde{\rho}_{ca} = \rho_{ca} e^{i\omega_L t}, \qquad \tilde{\rho}_{bc} = \rho_{bc} e^{-i\omega_L t}, \quad \tilde{\rho}_{cb} = \rho_{cb} e^{i\omega_L t}. \tag{3}$$

In the rotating-wave approximation, i.e., with neglect of terms oscillating at *double* the laser frequency, and upon adding relaxation terms, we then arrive at

$$\begin{aligned}
\dot{\rho}_{aa} &= \tfrac{1}{2} i\chi(\tilde{\rho}_{ac}\alpha - \tilde{\rho}_{ca}\alpha^*) - w(\rho_{aa} - \rho_{bb}) + k_c \rho_{cc} \ , \\
\dot{\rho}_{bb} &= \tfrac{1}{2} i\chi(\tilde{\rho}_{bc}\alpha - \tilde{\rho}_{cb}\alpha^*) - w(\rho_{bb} - \rho_{aa}) + k_c \rho_{cc} \ , \\
\dot{\tilde{\rho}}_{ac} &= \tfrac{1}{2} i\chi(\rho_{aa} - \rho_{cc} + \rho_{ab})\alpha^* + i\Delta_1 \tilde{\rho}_{ac} - T_2^{-1} \tilde{\rho}_{ac} \ , \\
\dot{\tilde{\rho}}_{ca} &= \tfrac{1}{2} i\chi(\rho_{cc} - \rho_{aa} - \rho_{ba})\alpha - i\Delta_1 \tilde{\rho}_{ca} - T_2^{-1} \tilde{\rho}_{ca} \ , \\
\dot{\tilde{\rho}}_{bc} &= \tfrac{1}{2} i\chi(\rho_{bb} - \rho_{cc} + \rho_{ba})\alpha^* + i\Delta_2 \tilde{\rho}_{bc} - T_2^{-1} \tilde{\rho}_{bc} \ , \\
\dot{\tilde{\rho}}_{cb} &= \tfrac{1}{2} i\chi(\rho_{cc} - \rho_{bb} - \rho_{ab})\alpha - i\Delta_2 \tilde{\rho}_{cb} - T_2^{-1} \tilde{\rho}_{cb} \ , \\
\dot{\rho}_{cc} &= \tfrac{1}{2} i\chi(\tilde{\rho}_{ca} + \tilde{\rho}_{cb})\alpha^* - \tfrac{1}{2} i\chi(\tilde{\rho}_{ac} + \tilde{\rho}_{bc})\alpha - 2k_c \rho_{cc} \ , \\
\dot{\rho}_{ab} &= \tfrac{1}{2} i\chi(\tilde{\rho}_{ac}\alpha - \tilde{\rho}_{cb}\alpha^*) + i\Delta\rho_{ab} - T_2'^{-1} \rho_{ab} \ , \\
\dot{\rho}_{ba} &= \tfrac{1}{2} i\chi(\tilde{\rho}_{bc}\alpha - \tilde{\rho}_{ca}\alpha^*) - i\Delta\rho_{ba} - T_2'^{-1} \rho_{ba} \ .
\end{aligned} \tag{4}$$

Here, $\alpha = e^{-i\mathbf{k}\cdot\mathbf{r} + i\phi}$ is a phase factor, and $\chi = \boldsymbol{\mu} \cdot \mathbf{E}_0/\hbar$, which measures the interaction strength of the laser field per optical transition, is the Rabi frequency. The off-

diagonal elements of the two optical transitions are assumed to decay with a single time constant T_2, and the off-diagonal elements connecting the two components of the ground-state decay with time constant T_2'. The decay rate k_c accounts for the radiative decay from the excited state to either ground state, and w for a mechanism equilibrating the populations within the ground state, which will be identified below as due to spin diffusion. Population decay within the ground state is ignored on account of its slow rate.[4]

Equations (4) can be rewritten in terms of a column vector $\rho = (\rho_{aa}, \rho_{bb}, \tilde{\rho}_{ac}, \tilde{\rho}_{ca}, \tilde{\rho}_{bc}, \tilde{\rho}_{cb}, \rho_{cc}, \rho_{ab}, \rho_{ba})$ and a 9×9 matrix M as

$$\dot{\rho} = -iM\rho \ , \tag{5}$$

which, if M is independent of time, has the formal solution

$$\rho(t) = \rho(0)e^{-iMt} \ . \tag{6}$$

The exponential of the matrix M has been evaluated for two cases: excitation field on, and excitation field off. We distinguish the two cases by the notations M' and M'', respectively. We further define the operators $A = \exp(-iM't)$ and $B = \exp(-iM''t)$. In the case of excitation field on, the exciting laser pulse is assumed to be short in comparison to all decays, and further so intense that $\Delta_1, \Delta_2 \ll \chi$. In other words, relaxation can be completely ignored, and Δ_1 and Δ_2 can be set to zero. To determine the operator A, then, we calculate the transformation matrix T which diagonalizes M', and subsequently evaluate

$$A = T^{-1}\left(e^{-i\lambda_j t}\delta_{jk}\right)T \ , \tag{7}$$

where λ_j are the eigenvalues of M'. The latter read

$$\lambda_{1,2} = \pm 2\theta, \quad \lambda_{3,4,5,6} = \pm\theta, \quad \lambda_{7,8,9} = 0 \ , \tag{8}$$

in which

$$\theta = \tfrac{1}{2}\sqrt{2}\int_0^\tau \chi(t)dt \tag{9}$$

is the pulse area of a laser pulse of width τ times a factor $\frac{1}{2}\sqrt{2}$ allowing for the fact that the available radiation energy has to be shared by the two optical transitions. The operator B, pertaining to the case of excitation field off, can be determined in the same manner, except that the eigenvalues λ_j read

$$\begin{aligned}
\lambda_1 &= -2iw \ , \\
\lambda_2 &= -2ik_c \ , \\
\lambda_{3,4} &= \pm i\Delta_1 - iT_2^{-1} \ , \\
\lambda_{5,6} &= \pm i\Delta_2 - iT_2^{-1} \ , \\
\lambda_7 &= 0 \ , \\
\lambda_{8,9} &= \pm i\Delta - iT_2'^{-1} \ .
\end{aligned} \tag{10}$$

The operators A and B are the implements to determine the development of the three-level system when subjected to any pulse sequence. Below, we employ them to calculate the accumulated-photon-echo signal.

B. Accumulated photon echo

The pulse sequence for accumulated photon echo is given in Fig. 1(b). First, we will examine the effect of a single pulse pair on the diagonal elements of the density matrix. The areas θ of both pulses are assumed equal, and much smaller than π. Directly after the second pulse ($t = t_{12}^+$), ρ is then given by

$$\rho(t_{12}^+) = A_2(\theta)B(t_{12})A_1(\theta)\rho(0) \ , \tag{11}$$

in which $A_1(\theta)$ and $A_2(\theta)$ refer to the pump and probe pulses, respectively. If all off-diagonal elements are taken to decay in the delay t_{23} prior to the next pulse pair, the effect of the pulse pair remaining after t_{23} is stored in the diagonal elements ρ_{aa}, ρ_{bb}, and ρ_{cc} of ρ. The associated 3×3 submatrix of $A_2(\theta)B(t_{12})A_1(\theta)$, for short denoted by A_2BA_1, has the structure given by

$$A_2BA_1\rho = \begin{pmatrix} 1-f_1-x & x & g_1 \\ x & 1-f_2-x & g_2 \\ f_1 & f_2 & 1-g_1-g_2 \end{pmatrix}\begin{pmatrix} \rho_{aa} \\ \rho_{bb} \\ \rho_{cc} \end{pmatrix} \ , \tag{12}$$

where f_1, f_2, g_1, g_2, and x all are much smaller than unity. The functions f_2 and g_2 are identical to f_1 and g_1, respectively, except for the replacement of Δ_1 by Δ_2, and vice versa. The contributions to lowest order in θ turn out to be the terms forming the optical population grating in the frequency domain. That is ($i = 1, 2$),

$$f_i = (1-\cos\theta)[\,2\cos(\Delta_i t_{12}^+ - \mathbf{k}_{12}\cdot\mathbf{r} + \phi_{12})e^{-t_{12}^+/T_2} + e^{-2k_c t_{12}^+} + 1] \ , \tag{13}$$

$$g_i = (1-\cos\theta)[\,2\cos(\Delta_i t_{12}^+ - \mathbf{k}_{12}\cdot\mathbf{r} + \phi_{12})e^{-t_{12}^+/T_2} + \tfrac{5}{2}e^{-2k_c t_{12}^+} - \tfrac{1}{2}] - \tfrac{1}{2}e^{-2k_c t_{12}^+} + \tfrac{1}{2} \ , \tag{14}$$

$$x = (\,1-\cos\theta)\left(e^{-2\omega t_{12}^+} - \tfrac{1}{2}e^{-2k_c t_{12}^+} - \tfrac{1}{2}\right) - \tfrac{1}{2}e^{-2\omega t_{12}^+} + \tfrac{1}{2} \ , \tag{15}$$

in which

$$\begin{aligned}
\mathbf{k}_{12} &= \mathbf{k}_1 - \mathbf{k}_2 \ , \\
\phi_{12} &= \phi_1 - \phi_2 \ .
\end{aligned} \tag{16}$$

Note that the grating, when integrated over the inhomogeneity of Δ_i, appropriately produces an echo at time t_{12} after excitation by the next pump pulse.[1] It furthermore is apparent that the two optical transitions develop independently of one another except for mixing by population transfer, as expressed by the parameter x. The latter encompasses the entire dependence on w, and obviously also contains a redistribution via optical pumping to $|c\rangle$ and subsequent reemission back to $|a\rangle$ and $|b\rangle$.

The effect of a sequence of successive pulse pairs, separated by t_{12} and following one another at intervals t_{23} [Fig. 1(b)], is accumulated over a time equal to the life-

time of the relevant level, which amounts to $(2k_c)^{-1} \approx 4$ ms for the excited state. As for the off-diagonal elements of ρ associated with the optical transitions (ρ_{ac}, ρ_{ca}, ρ_{bc}, and ρ_{cb}), fast optical dephasing ($T_2 < t_{23}$) as well as the dephasing by the displacements Δ_1 and Δ_2, ensure their complete decay before the next pulse pair is fired. The off-diagonal elements ρ_{ab} and ρ_{ba}, connecting the ground-state components, however, do not substantially decay within t_{23}, but do so over a number of pulse pairs. (A rough estimate of T_2' is 1 μs,[4] which is to be compared to $t_{12} + t_{23} = 12.2$ ns.) Their long-term effects furthermore average out well within the accumulation time, first, because of the small inhomogeneity of the ground-state splitting Δ, which leads to complete dephasing within at most a few μs, and, second, because the period $t_{12} + t_{23}$ of the pulse sequence is obviously incommensurable with $2\pi/\Delta$. Their effect on the grating buildup, therefore, is on the average independent of the initial values of the phases. To incorporate these approximations in a tractable way, transverse decay in the ground state (T_2') is ignored between pump and probe pulses, and assumed to be completed before the next pulse pair. Further justification for this procedure is found in the excellent agreement with experiment obtained below.

The steady-state grating, represented by ρ_{ss}, obeys [cf. Fig. 1(b)]

$$\rho_{ss} = B(t_{23})A_2(\theta)B(t_{12})A_1(\theta)\rho_{ss} \,, \tag{17}$$

in which the off-diagonal elements of ρ_{ss} are made to vanish. In Eq. (17), of course, the effect of the pumping is balanced by the decay. For a series of delays t_{12}, calculated values of the three population elements of ρ_{ss} pertaining to the $^4A_2$-$\overline{E}(^2E)$ transition in ruby are presented as a function of the detuning Δ_1 in Fig. 2 for the case $w \ll k_c$, and in Fig. 3 for $w \gg k_c$.

The signal intensity can now be determined by calculating the effect of the probe pulse on the excited-state population ρ_{cc}. Here, one should realize that excitation of the steady-state grating by the pump pulse invokes a macroscopic polarization interfering constructively with the probe pulse in both time and space, and that the release of the energy stored in ^2E results from *stimulated* emission from the excited state to the ground state at the time of the probe pulse. With the given scheme of modulation and detection, one thus has to calculate the change by the probe pulse of the cc component of ρ with the pump pulse on in comparison with the pump pulse off. The change of ρ_{cc} reflecting the detected signal intensity is then given by (Fig. 4)

$$\Delta\rho_{cc} = \left[A_2(\theta)B(t_{12}^+)A_1(\theta) - B(t_{12}^-)A_1(\theta)\right]_{cc} - \left[A_2(\theta)B(t_{12}^+) - B(t_{12}^-)\right]_{cc} \,,$$

which in the case of short pump and probe pulses (t_{12}^+, $t_{12}^- \approx t_{12}$) can be rewritten as

$$\Delta\rho_{cc} = \left\{[A_2(\theta) - I]B(t_{12})[A_1(\theta) - I]\rho_{ss}\right\}_{cc} \,. \tag{18}$$

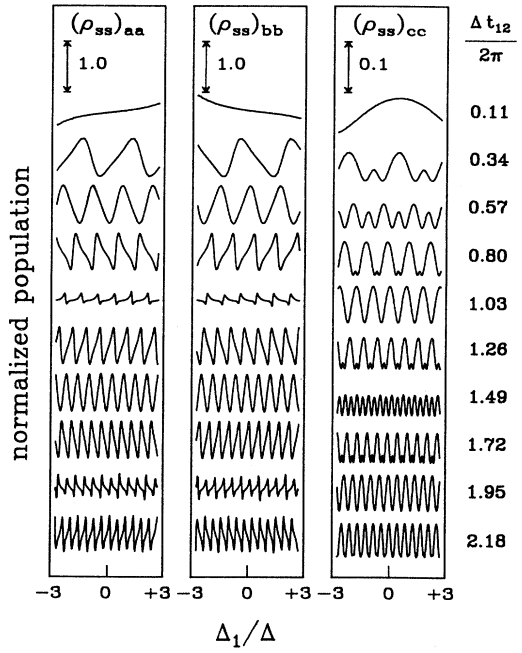

FIG. 2. The development of the steady-state spectral gratings with the delay in the absence of decay, as calculated from Eq. (17) for the case $w \ll k_c$. Detunings Δ_1 and delays t_{12} are in units Δ and $2\pi/\Delta$, respectively. The results apply directly to the $^4A_2$-$\overline{E}(^2E)$ transition in ruby, where $2\pi/\Delta = 87$ ps.

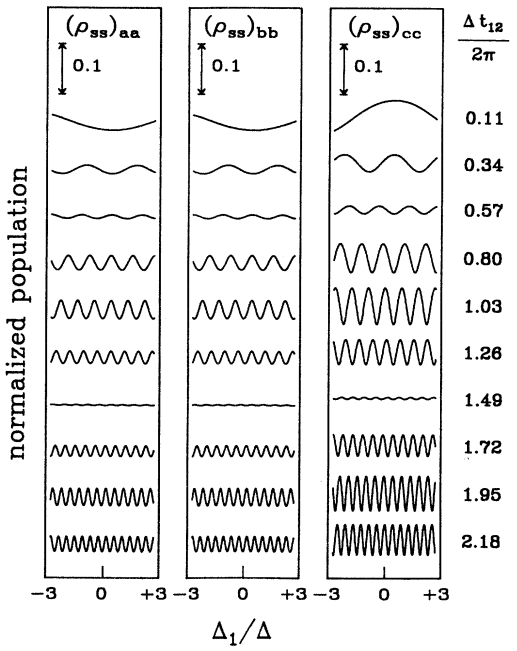

FIG. 3. Same as Fig. 2, but $w \gg k_c$.

The signal intensity subsequently follows from integration of this expression over the inhomogeneously broadened absorption line and the spatial phase. Results calculated by the use of Eq. (18) for the optical transition terminating in the $\overline{E}(^2E)$ level in ruby are presented in Fig. 5 for several values of w/k_c. In the case of small pulse areas and moderate decay rates, i.e.,

$$\theta^2 \ll wt_{23} \ll 1, \quad \theta^2 \ll k_c t_{23} \ll 1 , \tag{19}$$

the integral can be solved analytically, yielding for the signal intensity S_I to lowest order in θ

$$S_I \propto \frac{(1-\cos\theta)^2}{k_c(t_{12}+t_{23})}\left((1+\cos\Delta t_{12}) + \frac{k_c}{3w}(1-\cos\Delta t_{12})\right) e^{-2t_{12}/T_2} . \tag{20}$$

Note that Eq. (20) duplicates the essential features of Fig. 5. Also note that Eq. (20) returns to the standard nonoscillatory exponential decay with time constant $\frac{1}{2}T_2$ for vanishing Δ.

At this point, the role of w becomes apparent. In addition to the accumulated optical gratings, a grating is formed between the two components of the ground state. We first consider the limiting case where the integration time $(2w)^{-1}$ of the ground-state grating is large in relation to the integration time $(2k_c)^{-1}$ of the optical gratings ($w \ll k_c$, Fig. 2). The ground-state integration then dominates the signal intensity versus the delay despite the fact that the buildup of the ground-state grating is inherently less efficient. The ground-state grating, of course, develops its maximum depth at times $t_{12} = 2\pi(n+\frac{1}{2})/\Delta$, at which the two optical Bloch vectors interfere destructively. A pulse pair then excites only one of the optical transitions for a series of values of the absolute detuning Δ_1. Under these conditions, a substantial fraction of the population is transferred to the ground-state component that contributes most to the echo intensity since it is this component to which the Cr^{3+} ions return via the stimulated emission invoked by the probe pulse. At times of constructive interference ($t_{12} = 2\pi n/\Delta$), on the other hand, the two optical transitions behave similarly, and no ground-state grating is formed (cf. Fig. 2). Both transitions then contribute to the echo, although with a reduced amplitude because the integration time is now determined by k_c. In summing up the case $w \ll k_c$, we conclude the echo has maxima at $t_{12} = 2\pi(n+\frac{1}{2})/\Delta$, and minima at $t_{12} = 2\pi n/\Delta$. The other limiting case is where the communication among the ground-state components is so fast that no grating is formed between them ($w \gg k_c$). For all delays, the echo intensity then is determined by the optical gratings alone. This also results in a modulation of the echo intensity versus the delay, but one with the opposite phase since the buildup of the optical grating is at its maximum at times of constructive interference, and at its minimum at times of destructive interference (Fig. 3).

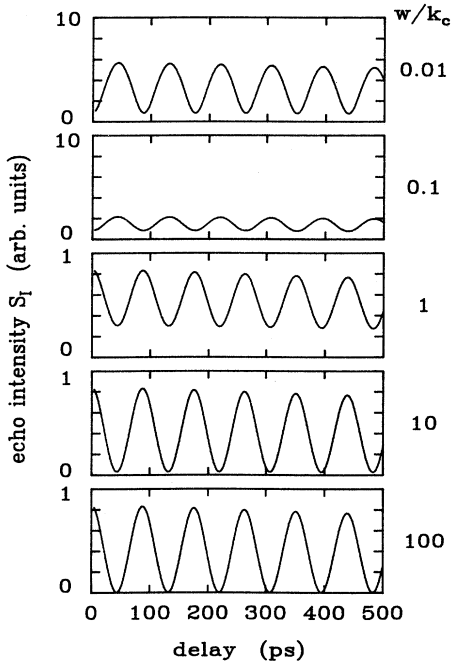

FIG. 5. The accumulated-photon-echo intensity vs the delay for the $^4A_2$-$\overline{E}(^2E)$ transition in ruby, calculated from the model described in the text for several values of w/k_c. The parameters are as follows: $\theta = 2\times10^{-4}$ rad, $k_c = 0.125$ ms^{-1}, $T_2 = 12$ ns, and $t_{12}+t_{23} = 12.2$ ns.

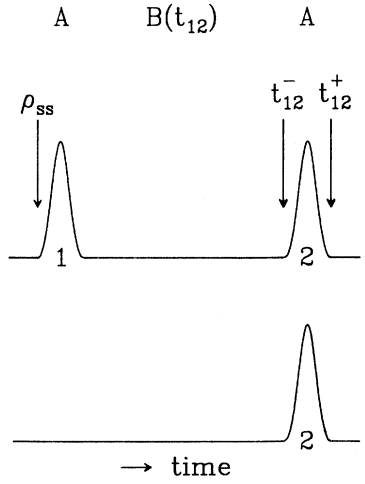

FIG. 4. The scheme to derive the echo intensity. The upper part represents the effect of a pump-probe pulse pair on the excited-state population at t_{12}^+ with reference to t_{12}^-, i.e., $A_2BA_1 - BA_1$. The lower part represents the effect of the probe pulse only, i.e., $A_2B - B$, which in the present modulation scheme of detection must be subtracted to obtain the signal intensity.

IV. RESULTS AND DISCUSSION

We present the results for the alexandrite sample in Fig. 6, and for the ruby sample in Fig. 7. The development of the accumulated photon-echo intensity of these Cr^{3+}-doped crystals with the delay of the probe pulse shows two distinct features. First, an overall decay occurs due to a loss of coherence with time. The ${}^4A_2$-$\overline{E}({}^2E)$ transitions (upper frames of Figs. 6 and 7) show only marginal dephasing in the present time window. This is consistent with earlier determinations of the homogeneous width of $\overline{E}({}^2E)$, which yielded T_2's of order 20 ns at temperatures sufficiently low for phonon-assisted processes to be frozen out.[5] The ${}^4A_2$-$2\overline{A}({}^2E)$ transitions, on the other hand, exhibit a significant loss of coherence, which obviously is associated with the transition from $2\overline{A}({}^2E)$ to $\overline{E}({}^2E)$ under the emission of a resonant phonon.[6] In fact, the decay time of the echo, half the dephasing time of $2\overline{A}({}^2E)$, equals the spontaneous phonon emission time T_1. This time is of significant interest because it governs the mean free path of resonant 29-cm^{-1} phonons against reabsorption by the $\overline{E}({}^2E)$-$2\overline{A}({}^2E)$ transition of Cr^{3+} in optically excited ruby,[7] and similarly 38-cm^{-1} phonons in alexandrite.[8] Second, the photon-echo signal exhibits an oscillatory dependence on the delay between the pump and probe pulses. The detailed calculations on the basis of the optical Bloch equations, presented in Sec. III, have made it evident that this beat is related to the ground-state splitting.

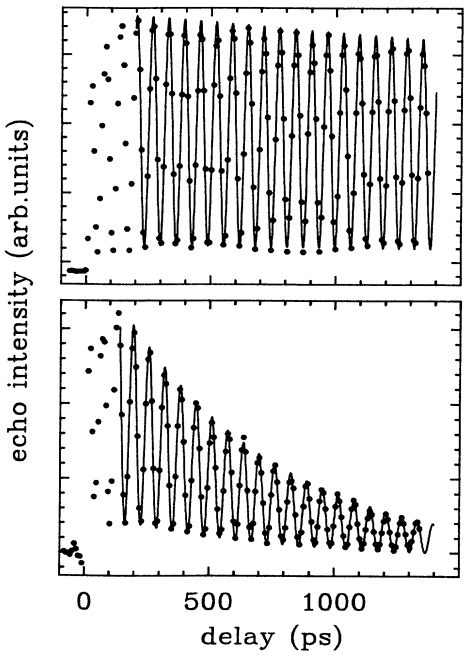

FIG. 6. The accumulated-photon-echo intensity vs the delay for the ${}^4A_2$-$\overline{E}({}^2E)$ and ${}^4A_2$-$2\overline{A}({}^2E)$ transitions (upper and lower frames, respectively) in 2000-at. ppm alexandrite. The solid curves are fits to the data.

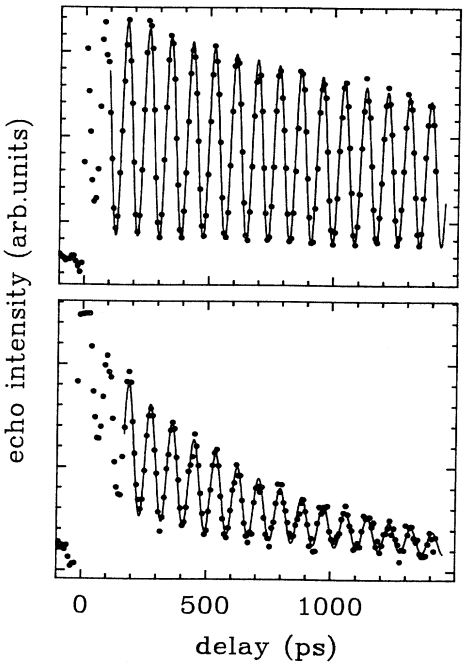

FIG. 7. Same as Fig. 6, but in 700-at. ppm ruby. The solid curves are fits to the data.

As can be seen from Eq. (20), the beat is made up of two contributions which are of opposite phase with mutual weights determined by w/k_c. Inspection of the experimental data for the ${}^4A_2$-$\overline{E}({}^2E)$ transition immediately shows that the first term in Eq. (20) predominates in both alexandrite and ruby, so the experiments indicate that $w/k_c \gg 1$. The dependence of the echo intensity as it results from regular dephasing and the ground-state splitting combined [Eq. (20)] has been fitted to the data of the $2\overline{A}({}^2E)$ echoes, and, although their decay is minimal, to the $\overline{E}({}^2E)$ echoes, with T_2, Δ, w/k_c, and an overall prefactor as variables. The result for the $\overline{E}({}^2E)$ echo results in the estimate that w/k_c is at least of order 10 (cf. Fig. 5). It should be noted, however, that this is a lower limit because any differences in the probabilities of the ${}^4A_2(M_S=\pm\frac{3}{2})$-$\overline{E}({}^2E)$ and the ${}^4A_2(M_S=\pm\frac{1}{2})$-$\overline{E}({}^2E)$ transitions, not accounted for in the derivation of Eq. (20), would also show up as a decrease of the beat depth. After averaging over several decays such as the ones in Figs. 6 and 7, the results for $T_1 = \frac{1}{2}T_2$ and Δ are tabulated in Table I. We note that the results for T_1 compare with the result $T_1 = 0.66 \pm 0.04$ ns for ruby and $T_1 = 0.54 \pm 0.05$ ns for alexandrite from a recent study of the $\overline{E}({}^2E)$ and $2\overline{A}({}^2E)$ line shapes with fluorescent line narrowing.[9]

The most likely mechanism responsible for communication among the two components of the ground state is spin diffusion, such as invoked by dipolar interactions.[4] Consider a number of Cr^{3+} centers with matching ground-state splittings, but different optical splittings. In systems diluted to, say, 1000 at. ppm, typical times for a diffusive step, i.e., a transition $|a\rangle \rightarrow |b\rangle$ on one site

TABLE I. Decay time T_1 of $2\overline{A}(^2E)$ and zero-field splitting Δ of $^4A_2$ of Cr^{3+} in ruby and alexandrite.

	Ruby	Alexandrite
T_1 (ns)	0.70 ± 0.05	0.63 ± 0.05
Δ (cm^{-1})	0.383 ± 0.001	0.526 ± 0.002

and an associated transition $|b\rangle \rightarrow |a\rangle$ on the next, are of the order 1 μs,[4] so in the typical integration time of the experiment the distance covered is at least of the order of a micrometer. Note that spin diffusion is slow compared to all dephasing times. The essential reason why ground-state diffusion affects the gratings is that with each step it effectively modifies Δ_1 because of the significant inhomogeneity existing in the *optical* transition. For each Δ_1, of course, the centers satisfy a set of equations of motion such as Eqs. (4). Therefore, while spin diffusion does not change the total populations of $|a\rangle$ and $|b\rangle$, it tends to average out the $|a\rangle$ and $|b\rangle$ population gratings (Fig. 3). More precisely, only those fractions of the $|a\rangle$ and $|b\rangle$ population gratings remain that have equal phases with reference to the respective optical transitions. This, indeed, is precisely what is seen if we go from Fig. 2 for $w \ll k_c$ to Fig. 3 pertaining to the limit of very strong population transfer within the ground state. In this context it is noted that the phase of the respective optical transitions, $\Delta_i t_{12} - \mathbf{k}_{12} \cdot \mathbf{r} + \phi_{12}$, is predominantly governed by the part $\Delta_i t_{12}$, at least for times exceeding the reciprocal spread of the line, i.e., the optical inhomogeneous dephasing time T_2^*. The spatial part of the phase varies only slowly, having a period of ~ 10 μm for the relevant crossing angle of the input beams. For times $t_{12} < T_2^*$, the inhomogeneous optical line is not wide enough to contain more than a single period $2\pi/t_{12}$ of the grating. The excitation accordingly has to cover a significant distance for the grating to be disrupted. This point is confirmed from a comparison of the first minima of the echo intensity of the $\overline{E}(^2E)$ echo in alexandrite and ruby (Fig. 8 shows enlargements of the relevant portions of Figs. 6 and 7). In alexandrite, T_2^* is very short (5 ps) and the minima have reached a constant level, whereas in ruby the first minima drop with a time constant which within errors corresponds to $T_2^* \approx 80$ ps.

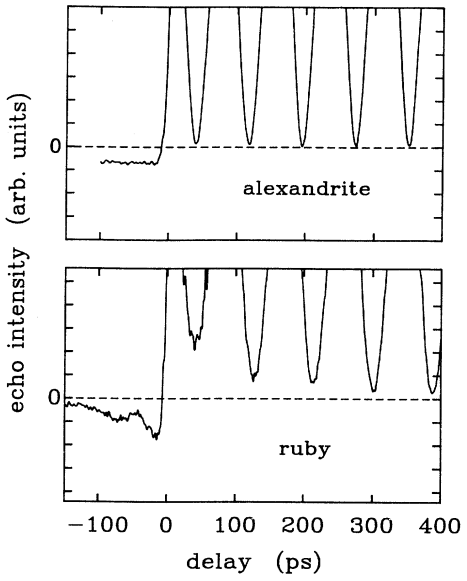

FIG. 8. The initial development of the minima in the accumulated-photon-echo intensity vs the delay in alexandrite and ruby, demonstrating the effect of spin diffusion within the ground state.

V. CONCLUSIONS

In conclusion, we have measured, in the time domain, the homogeneous dephasing times of the $^4A_2$-$2\overline{A}(^2E)$ transition of Cr^{3+} in ruby and alexandrite. We further have demonstrated that the technique of accumulated photon echo allows us to extract level splittings with high accuracy via the beat which they produce in the echo intensity versus the delay. The phase and amplitude of this beat demonstrate that spin diffusion in the ground state is rapid compared to the radiative decay rate of the ^2E levels. We finally note that we have recently used the technique of accumulated photon echo to measure the pressure dependence of the ground-state splitting in ruby at 10 K under hydrostatic pressures up to 4.3 GPa.[10]

ACKNOWLEDGMENTS

The authors thank C. R. de Kok for excellent technical assistance. The work was financially supported by the Netherlands Foundation Fundamenteel Onderzoek der Materie (FOM) and the Nederlandse Organisatie voor Wetenschappelijk Onderzoek (NWO).

[1] W. H. Hesselink and D. A. Wiersma, Phys. Rev. Lett. **43**, 1991 (1979).
[2] S. Sugano and Y. Tanabe, J. Phys. Soc. Jpn. **13**, 880 (1958).
[3] M. D. Levenson, *Introduction to Nonlinear Laser Spectroscopy* (Academic, New York, 1982).
[4] R. L. Kyhl and B. D. Nagewara-Rao, Phys. Rev. **158**, 284 (1967).
[5] P. E. Jessop, T. Muramoto, and A. Szabo, Phys. Rev. B **21**, 926 (1980); V. A. Zuikov and V. V. Samartsev, Phys. Status Solidi A **73**, 683 (1982).
[6] M. Blume, R. Orbach, A. Kiel, and S. Geschwind, Phys. Rev. **139**, A314 (1965).

[7] For a review see K. F. Renk, in *Nonequilibrium Phonons in Nonmetallic Crystals*, edited by W. Eisenmenger and A. A. Kaplyanskii (North-Holland, Amsterdam, 1986), p. 317.
[8] R. J. G. Goossens, J. I. Dijkhuis, and H. W. de Wijn, in *Phonon Scattering in Condensed Matter*, edited by W. Eisenmenger, K. Lassmann, and S. Döttinger (Springer-Verlag, Berlin, 1984), p. 12.
[9] M. J. van Dort, M. H. F. Overwijk, J. I. Dijkhuis, and H. W. de Wijn, Solid State Commun. **72**, 237 (1989).
[10] M. H. F. Overwijk, J. I. Dijkhuis, H. W. de Wijn, R. Vreeker, R. Sprik, and A. Lagendijk, *Conference on Quantum Electronics and Laser Science 1989, Technical Digest Series* (Optical Society of America, Washington, D.C., 1989), Vol. 12, p. 252; Phys. Rev. B **43**, 12 744 (1991).